

Extending Semantic Edge Labelling

Guanghua Zhang and Andrew Wallace
Department of Computing and Electrical Engineering
Heriot-Watt University
Edinburgh EH14 4AS, Scotland
guanghua, andy@cee.hw.ac.uk

Abstract

In earlier work [9, 10], we developed an approach to edge labelling and depth reconstruction based on fusion of registered depth and intensity images. This paper presents a new method and extensions to the first stage of that approach, that is the detection and semantic labelling of the edge data. Reflectance edges are extracted from an intensity image, and quadratic curves are fitted to range and intensity data along each row and column using an intensity guided splitting and merging process. Edge labels are determined by examination of the changes in depth, surface orientation and intensity at each edge site.

1 Introduction

There has been considerable recent interest in combining data from multiple data sources [3], most commonly registered range and reflectance data from the same scene [6, 7, 10]. This can lead to a more reliable, accurate and complete description of the scene in terms of both the geometry and the surface characteristics. In our case, it allows a semantic labelling of the boundaries in the scene, either locally [10] or in extended form [8]. As an adjunct to this process, we can also produce a reconstructed depth image [10], leading to an improved surface segmentation.

In this paper, we present initial results of a new approach to semantic edge labelling which extends our earlier work to provide a more complete set of edge labels. We replace the previous edge detection process by an intensity-guided splitting and merging algorithm to fit planar and quadratic segments to depth and intensity data and define sites of discontinuity. This has two advantages. First it allows a more complete classification of edge type by examination of the adjacent surfaces. Second, it forms a pre-processing step for depth segmentation or reconstruction by grouping adjacent row and column segments. We illustrate the approach by some experimental results from both synthetic and real data.

2 Combining Range and Intensity Data to Label Edges

Given accurate and complete knowledge of the lighting configuration and a model of the angular distribution of the surface reflectance, it is possible to deduce the scene geometry and the magnitude of the surface reflectance from depth and intensity data using an exact quantitative shading model [7]. This is a powerful approach, but is less applicable to the general case when the surface reflectance model and lighting positions are unknown. In this paper we adopt a more qualitative approach.

Previous approaches to the fusion of range and intensity data were based on pixels [1, 10]. Although suitable for describing scenes having general surfaces, application of strong constraints on surface shape allows a more robust form of discontinuity detection. In this work, we adopt a quadratic surface model for range and intensity data.

Our previous work [10] dealt with four semantic edge labels: *blade/extremal*, *fold*, *mark/specular/shadow* and *no-edge*. Here, we wish to extend this to a fuller set of edge labels. A qualitative description of the anticipated changes in depth, orientation and intensity, together with the adjacent surface characteristics is given in Table 1.

Label	Changes		Adjacent Surface Characteristics
Blade	depth gradient intensity	Yes Possible Probable	Smooth surfaces, planar or curved. Planar and constant intensity, or curved and varying intensity.
Extremal	depth gradient intensity	Yes Yes Probable	Smooth surfaces, at least one curved. Normal of curved surface orthogonal to viewing angle adjacent to edge. Variation of intensity on curved surface.
Fold	depth gradient intensity	No Yes Probable	Smooth surfaces, planar or curved. Planar and constant intensity, or curved and varying intensity.
Mark	depth gradient intensity	No No Yes	Smooth surfaces, no change in depth profile. Sharp discontinuity in intensity within smooth intensity variation.
Shadow	depth gradient intensity	No No Yes	Smooth surfaces, no change in depth profile. Blurred or sharp (light dependent) One dark region adjacent to edge.
Specular	depth gradient intensity	No No Yes	Smooth surfaces, no change in depth profile. A bright region adjacent to edge, with bell-shaped intensity profile. Probable curved but possible planar surface.
No edge	depth gradient intensity	No No No	No change in any properties.

Table 1: Classification of edges with semantic labels.

2.1 Initial 1D curve fitting

We apply a one dimensional splitting and merging algorithm to each row and column of each image. The initial break points are defined by peaks in the output of a Canny edge operator applied to the intensity data. These estimates are used to subdivide rows and columns for the first iteration of the fitting algorithm. From Table 1 we note that it is probable that geometric discontinuities will result in intensity changes, but that intensity changes need not have corresponding changes in depth, for example at mark boundaries. Incorrect initial break points in the depth data are eliminated subsequently by the merging process. The algorithm is defined below; the input images are assumed to be contaminated by Gaussian noise with a small proportion of outliers, the resulting output is a linked list for each row and column of each image. The linked lists define the parameters of each 1D curve segment, separated by the coordinates defining the break points in each row or column. This method is fast and produces more accurate results when compared with alternative methods [5].

Input : Intensity, depth and edge (intensity) images

Parameters:

T_{break} : the largest depth/intensity difference on a curve

T_{fit} : acceptable least square fitting error

Output : linked lists along rows and columns, each curve is described by a linear or quadratic equation: $z = a_1x + a_0$ or $z = a_2x^2 + a_1x + a_0$

Begin:

For each intensity and range image

For each row and column

Construct a list of segments bounded by intensity edge points

For each segment

Repeat

Construct a straight line connecting the two end points

Search for the largest distance d_{max} from the segment

points to this line, note it as potential break point

Fit a linear and a quadratic curve to the segment

If $d_{max} < T_{break}$ and linear fit error smaller than T_{fit}

Then accept linear fit

Else If quadratic fit error smaller than T_{fit}

Then accept quadratic fit

Else split the segment into two at break point

Endif

Endif

Until all segments are fitted

Endfor

Endfor

Endfor

End

2.2 Edge Classification

A multiple level classification tree is used for the initial classification of edge labels. We wish to determine the type of edge from prototypical behaviour summarised in Table 1. Currently, this is implemented in the form of a decision tree. Not all behaviours summarised in Table 1 are implemented. Those which are not used at present are italicised in Levels 1 and 2. No distinction is made currently at Level 3.

Level 1:

At the first level, we distinguish blade/extremal from fold, mark, shadow and specular on the basis of the most significant factor, the change in depth across the edge. If a significant change in depth occurs, the discontinuity is either a blade or extremal edge.

Level 2:

At the second level, an edge is labelled as extremal, rather than blade, if

- at least one depth function, $z(x)$, is quadratic.
- $\text{atan}(d'(x)) \approx \pi/2$ adjacent to the boundary.
- *if light source and viewing direction adjacent, $I(x)$ approaches to ambient reflectance level and $\text{atan}(I'(x)) \approx \pi/2$*

These values are computed from the the location of the edge and the coefficients of the adjacent segments.

At the second level, an edge is labelled as fold rather than mark/shadow/specular on the basis of the change in orientation of the adjacent segments; the orientation adjacent to the boundary is again calculated from the location and segment coefficients in the depth data. If a significant change in orientation is observed then the edge is labelled as a fold edge. This is confirmed by the probable presence of a discontinuity in the intensity data.

Level 3:

This represents the most difficult part of the process, distinguishing between the several types of discontinuity in the intensity function when no discontinuity is observed in depth or orientation. This part of the labelling process can be eased by knowledge of the light source position.

To distinguish specular edges, we determine whether the image data exhibit the following characteristics, again determined from the list structure.

- the depth function $z(x)$ is usually quadratic.
- generally the specular region is between two specular edges.
- generally the specular region has a quadratic (bell-shaped, high curvature) profile.
- the intensity function is much higher than the local mean.

If we have knowledge of the light source direction and distribution,

- at the centre of the specular region (between the edges) the normal bisects the light source and viewing directions.
- if the light is diffuse, specularities occur only at high curvatures.

Distinguishing shadow from mark edges is difficult. If no global context is present it may be impossible to do so. In a single image, we anticipate the following

- a mark is generally a sharp discontinuity, a shadow may be sharp or blurred. Hence we can refit an edge profile across the edge to determine this.
- a shadow edge will generally have an adjacent intensity function, $I(x)$, which is much lower than the local mean. This *may* be the case with a mark.

If we can constrain the problem by knowledge of the light source

- if the position of a point-like source is known we may be able to find an occluding edge in the data which lies on the line from the shadow to the source. (This may be outwith the image)
- if the light and view are coincident the image is shadowless.
- if the light is diffuse the shadows are blurred.

Combining the above rules, we achieve edge classification from the linked edge lists.

Edge labels L : [*blade, fold, extremal, mark/specular/shadow, null*]

Input : linked curve lists of intensity and depth data (rows and columns)

Output : dual lattice representation of initial edge labelling

Begin:

Traverse both linked intensity and depth curve lists

For each edge site in either list

 Extract the value, $z(x)$, and gradient, $z'(x)$, of adjacent curves

 Compute changes in depth, surface orientation and intensity

 Classify edge into one of the edge labels

Endfor

Endtraverse

End

To classify the several edge labels based on the several discontinuities, we use a maximum likelihood estimator,

$$\frac{P(L = \text{edge} \mid \delta)}{P(L = \text{null} \mid \delta)} = \frac{P(\delta \mid L = \text{edge})P(L = \text{edge})}{P(\delta \mid L = \text{null})P(L = \text{null})} > 1 \quad (1)$$

Assuming the presence of Gaussian noise with standard deviation σ , we have the following probabilities [4]:

$$P(\delta | L = null) = \exp[-(\delta/\sigma)^2] \text{ and } P(\delta | L = edge) = 1 - \exp[-(\delta/\sigma)^2] \quad (2)$$

We obtain the following condition for assigning an edge label

$$\delta > \sigma \sqrt{-\ln(P(L = edge))} \quad (3)$$

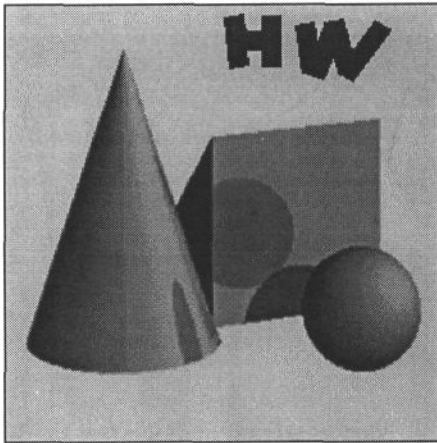
Additional information can be obtained either by variation of the light source or viewing direction to obtain two images. Two or more images may be acquired from different viewpoints. In this case, the visible marks should not change. The shadow edges should not change. However, the position of the specular edges should change. If a point-like light source is moved, both the shadow and specular edges will, in general, change position. If the object is moved, both the shadow and specular edges will, in general, change position.

3 Experimental results

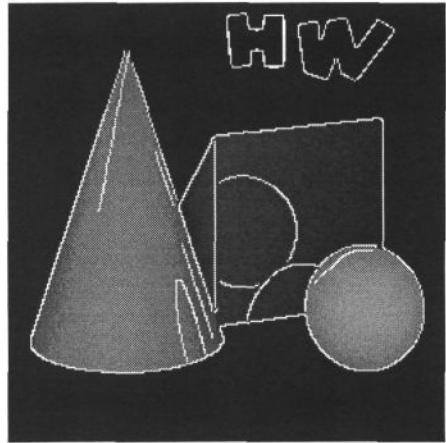
The algorithm has been tested on both synthetic and real image data. Throughout all the experiments, edge classification occurs at intensity edge location. A pair of registered synthetic range and intensity data, illustrated in Figure 1 (a) and (b), is generated using a raytracing program with Gaussian noise added (standard deviation 2.0). The classified edge labels are shown in Figure 1 (c) to (f). Blade and extremal labels can be mixed as the quadratic surface model is inappropriate for describing circular shape resulting fragmentation and the tangential angle at the edge site is far from 90°. This happens at extremal edges of the cone, where most extremal edges are detected correctly along each row, however, some of them are classified as blade along columns. A solution to this problem is to refit a suitable model to a segment at later stage. An example of this fragmentation and depth reconstruction from curve fitting is shown in Figure 2. In Figure 2(b), the breakpoints are marked by null pixel values.

Another example is illustrated in Figure 3, in which the data were acquired from the ABW range sensor ¹. Figure 3 (a) and (b) show the registered intensity and range data, and Figure 3 (c) shows the detected intensity edges. As there are no mark and extremal edges present, only the extracted blade and fold edge labels are displayed in Figure 3(d) and (e). Almost all the blade and extremal edges are detected correctly. However, due to the uniform colour of the polyhedras and the background and location of the lighting source, some intensity edges are missed causing edges at these locations to be unclassified. These edges are still picked up by the curve fitting process as shown in the reconstructed depth data, Figure 3(f). Depth profiles along row 260 in the original and the reconstructed range data are shown in Figure 4.

¹We acknowledge the use of ABW range data which is available from <http://marathon.csee.usf.edu/range/seg-comp/images.html>



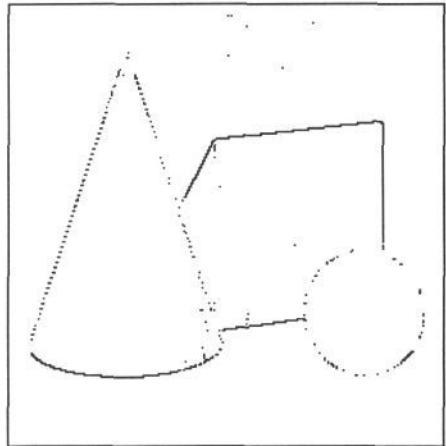
(a) intensity image



(b) range image with intensity edges



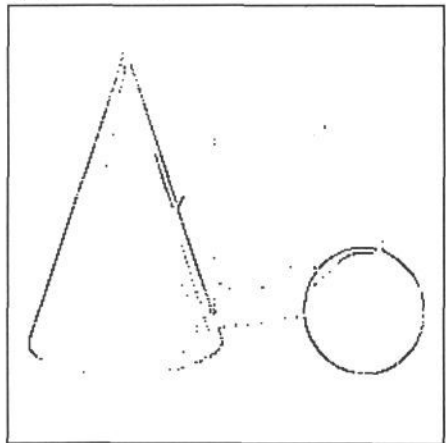
(c) mark edges



(d) blade edges



(e) fold edges



(f) extremal edges

Figure 1: Results from a pair of synthetic intensity and range images.

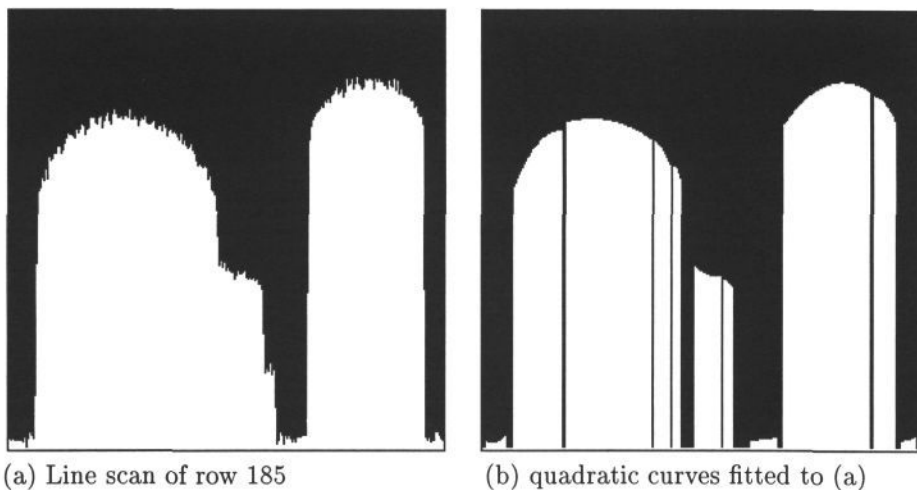


Figure 2: Results from a pair of synthetic images.

4 Discussion

We have presented preliminary results from a new approach to extend the definition of semantic edge labels from registered range and intensity images. This is different from current methods in that preprocessing of intensity and range data into 1D segments provides not only the information about the changes in depth, normal and reflectance, but also the profile of the adjacent surfaces. This is very important in distinguishing certain edge and surface types, and in choosing an appropriate surface model for surface parameter extraction.

By combining range and intensity data of the same scene, we make full use of the information available from a range sensor. Thus, we aim to simplify the subsequent segmentation processes and improving the system robustness. However, we have not yet incorporated the full set of characteristic behaviours into the primary classification process. Nor do we anticipate that the primary process represents a completion of the task; we intend to adapt existing algorithms to update the edge labels on the basis of local continuity and consistency [10], and to show how the 1D segments can be grouped directly to form surface patches in 2D, (as opposed to reconstruction and segmentation of reconstructed 2D data [10]). Finally, we shall apply these algorithms to images taken from existing sensors to obtain multiple registered depth and intensity images [2].

5 Acknowledgement

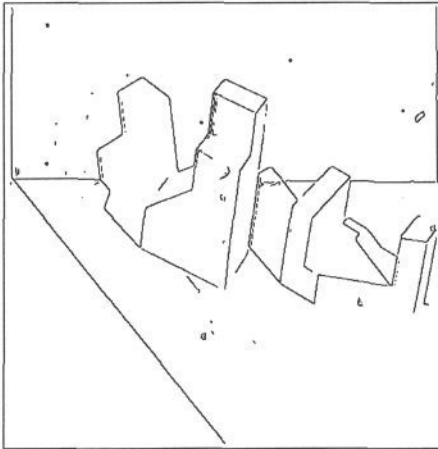
The work is supported by UK EPSRC Grant (NO. GR/J07891): Part Identification and Positioning by Sensor Fusion.



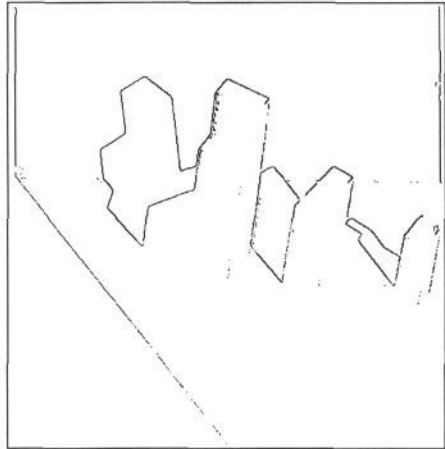
(a) intensity image



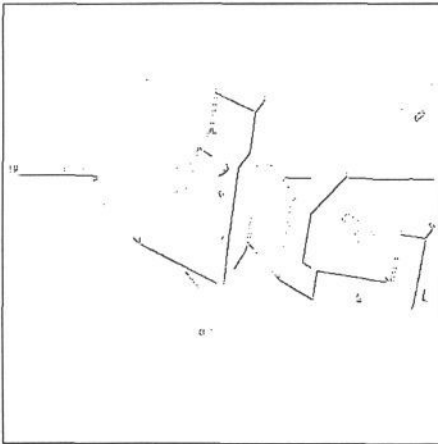
(b) range image



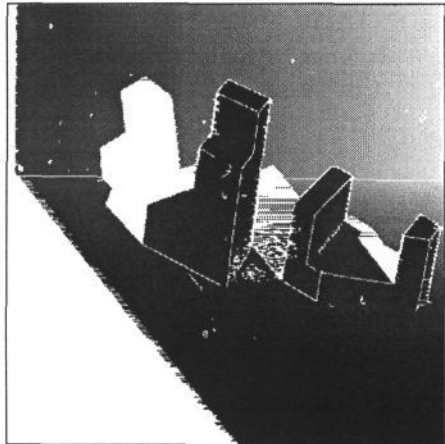
(c) intensity edges



(d) blade edges



(e) fold edges



(f) reconstructed depth

Figure 3: Results from a pair of ABW intensity and range images.

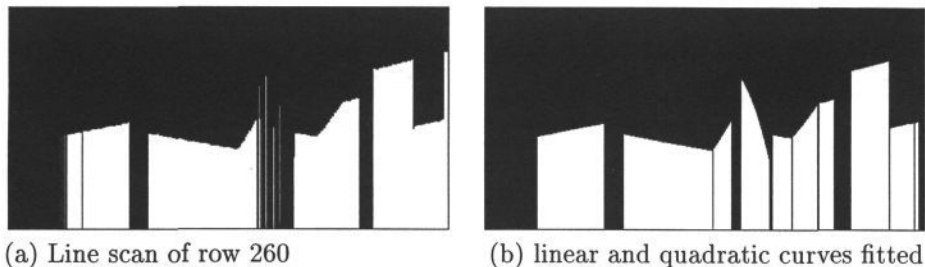


Figure 4: Results from a pair of real range and intensity images.

References

- [1] P. B. Chou and C. M. Brown. The theory and practice of Bayesian image labeling. *Int. J. Comput. Vision*, 4:185–210, 1990.
- [2] J. Clark and A. M. Wallace. Depth sensing by variable baseline triangulation. *submitted to British Machine Vision Conference*, 1995.
- [3] J. K. Hackett and M. Shah. Multi-sensor fusion: a perspective. In *Proc. IEEE Int. Conf. Robotics and Automation*, pages 1324–1330, 1990.
- [4] E. R. Hancock and J. Kittler. Edge-labeling using dictionary-based relaxation. *IEEE Trans. Pattern Anal. Mach. Intel.*, 12(2):165–181, 1990.
- [5] A. Hoover, G. Jean-Baptiste, X. Jiang, P. J. Flynn, H. Bunke, D. Goldgof, and K. Bowyer. A comparison of range image segmentation algorithms. *submitted to Proc. Int. Conf. Computer Vision*, 1995.
- [6] G. Kay and T. Caelli. Inverting an illumination model from range and intensity maps. *CVGIP: Image Understanding*, 59(2):183–201, 1994.
- [7] H. D. Tagare and R. J. P. deFigueiredo. A framework for the construction of reflectance maps for machine vision. *CVGIP: Image Understanding*, 57(3):265–282, 1993.
- [8] G. Zhang, E. Thirion, and A. M. Wallace. Model matching using multiple data sources. In F. Y. Wu and B. M. Dawson, editors, *Machine Vision Applications in Industrial Inspection*, volume Proc. SPIE 1907, pages 2–12, 1993.
- [9] G. Zhang and A. M. Wallace. Edge labelling by fusion of intensity and range data. In P. Mowforth, editor, *Proc. British Machine Vision Conf.*, pages 412–415, 1991.
- [10] G. Zhang and A. M. Wallace. Physical modelling and combination of range and intensity edge data. *CVGIP: Image Understanding*, 58(2):191–220, 1993.